CHEMISTRY
AN ASIAN JOURNAL
www.chemasianj.org

Accepted Article

Title: Efficient Nondoped Pure Blue Organic Light Emitting Diodes Based on Anthracene and 9,9-Diphenyl-9,10-dihydroacridine Derivative

Authors: Ping Lu, Xin He, Shenghong Ren, Hui Liu, Shiyuan Zhao, Futong Liu, Chunya Du, Jiarui Min, and Haiquan Zhang

To be cited as: *Chem. Asian J.* 10.1002/asia.201901376

Link to VoR: http://dx.doi.org/10.1002/asia.201901376

A Journal of
ACES Asian Chemical Editorial Society

A sister journal of Angewandte Chemie and Chemistry – A European Journal

WILEY-VCH

10.1002/asia.201901376

WILEY-VCH

Efficient Nondoped Pure Blue Organic Light Emitting Diodes Based on Anthracene and 9,9-Diphenyl-9,10-dihydroacridine Derivative

Xin He+,[a] Shenghong Ren+,[a] Hui Liu,[a] Shiyuan Zhao,[a] Futong Liu,[a] Chunya Du,[a] Jiarui Min, [b] Haiquan Zhang*,[b] and Ping Lu*,[a]

Dedication ((optional))

Abstract: Organic light emitting diodes (OLEDs) have been greatly developed in recent years owing to their abundant advantages for full-color displays and general-purpose lightings. Blue emitters not only provide one of the primary colors of the RGB (red, green and blue) display system to reduce the power consumption of OLEDs, but also are able to generate light of all colors, including blue, green, red, and white by energy transfer processes in devices. However, it remains challenge to achieve high-performance blue electroluminescence, especially for nondoped devices. In this paper, we report a blue light emitting molecule, DPAC-AnPCN, which consists of 9,9-diphenyl-9,10-dihydroacridine and p-benzonitrile substituted anthracene moieties. The asymmetrically decoration on anthracene with different groups on its 9 and 10 positions combines the merits respective constructing units and endows DPAC-AnPCN with pure blue emission, high solid-state efficiency, good thermal stability and appropriate HOMO and LUMO energy levels. Furthermore, DPAC-AnPCN can be applied in nondoped device to effectively reduce the fabrication complexity and cost. The nondoped device exhibits pure blue electroluminescence (EL) locating at 464 nm with CIE coordinates of (0.15, 0.15). It also can keep high efficiency at relatively high luminescence. The maximum external quantum efficiency (EQE) reaches 6.04% and still remains 5.31% at the luminance of 1000 cd m^{-2} showing a very small efficiency roll-off.

Introduction

Organic light emitting diodes (OLEDs) have progressed rapidly since its first discovery by C. W. Tang and VanSlyke in 1987 for their promising applications as solid-state lighting sources and full-color displays.[1] Although some OLEDs products in flat-panel display fields such as mobile phones and televisions have been commercially available in recent years, there still exists several bottlenecks for their wide applications. A critical one is the lack of highly efficient blue materials.[2] Blue emission not only represents one of the primary colors of the RGB (red, green and blue) display system to effectively reduce the power consumption of devices, but also serves as host materials for other low energy dopants to fabricate RGB/white OLED devices by energy transfer process.[3] In particular, the performance of pure blue materials is far from satisfaction in terms of device efficiency and stability for commercialization as compared with their red and green counterparts.[4] Therefore, developing blue emitting materials with high efficiency is of significant importance. Traditional blue fluorescent materials can only provide limited EQE because they can only use singlet excitons, which constitutes 25% electrically generated excitons according to the electron spin statistics, to emit fluorescence.[5] In order to break through the predicament, phosphorescent materials based on Ir or Pt heavy metals are extensively developed which can harvest both singlet and triplet excitons to achieve hundred percent internal quantum efficiency (IQE). But these unsustainable phosphorescent complexes are rather expensive and noxious which also hampers their long-term application.[6] Thermally activated delayed fluorescence (TADF) is another effective way to attain 100% IQE though reverse intersystem crossing (RISC) process from lowest triplet excited state (T_1) to the lowest singlet excited state (S_1).[7] However, OLEDs based on these two kinds of materials often needs to be doped into proper host materials with appropriate doping concentration to get ideal device performances.The doping strategy will complicate the device fabrication procedures and increase the device cost.[8] In addition, they also suffer from varying degrees of efficiency roll-offs caused by triplet-triplet quenching at high luminescence, which is an obstacle for their applications.[9] Recently, many researchers endeavor to develop pure organic blue materials for nondoped devices.[10] These materials with no TADF property achieve appreciable device performance with high luminance and ideal efficiency roll-off. But the EQE of these fluorescent materials are not comparable and the material structures are limited to several aromatic fused rings, which hinder the development of nondoped blue devices. Therefore, the developing of pure organic blue materials with high efficiency and novel molecular structure which is designed for nondoped

[a] *Dr. X. He, Dr. S. Ren, Dr. H. Liu, Dr. S. Zhao, Dr. F. Liu, Dr. C. Du, Prof. P. Lu*
Department of Chemistry
Jilin University
State Key Laboratory of Supramolecular Structure and Materials
2699 Qianjin Avenue, Changchun 130012 (P. R. China)
E-mail: lup@jlu.edu.cn

[b] *Dr. J. Min, Prof. H. Zhang*
Yanshan University
State Key Laboratory of Metastable Materials Science and Technology
E-mail: hqzhang@ysu.edu.cn

[+] *These authors contributed equally to this work.*

device retains great significance for both science research and practical applications.

In this work, DPAC-AnPCN is reported as a highly efficient blue-emitting material which is constructed by connecting 9,9-diphenyl-9,10-dihydroacridine (DPAC) with p-benzonitrile substituted anthracene. Anthracene is an efficient chromophore of blue fluorescence with high photoluminescence quantum yield (PLQY) owing to its rigid planar structure.[11] Besides, anthracene has two reaction sites on its 9 and 10 positions, so that asymmetrically decoration on anthracene with different groups can be realized. Further, anthracene possesses appropriate wide bandgap which ensures the blue emission of its derivatives.[12] DPAC is introduced as a weak electron donor group which is connected with anthracene through a bridging benzene. DPAC has higher highest occupied molecular orbital (HOMO) than anthracene to effectively reduce hole injection barrier in its devices.[13] On the other site of anthracene, p-benzonitrile group is introduced as electron-withdrawing group which can lower the LUMO energy level of target molecule to reduce electron injection barrier and modify the emission wavelength. As a result, 4-(10-(4-(9,9-diphenylacridin-10(9H)-yl)phenyl)anthracen-9-yl)benzonitrile (DPAC-AnPCN) is successfully achieved which exhibits blue emission with high PLQY of 65% in its pure film. Especially, the non-doped OLED using DPAC-AnPCN as the active layer shows the maximum EQE of 6.04% with EL peak of 464 nm and a very low efficiency roll-off. The CIE coordinates locate at (0.15, 0.15), which matches well with the criteria of pure blue OLEDs.

Results and Discussion

Synthetic procedures

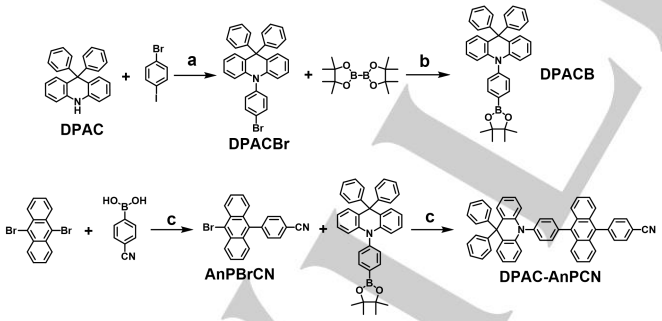

Scheme 1. Synthesis route of DPAC-AnPCN. a) Ullmann coupling reaction: CuI, trans-1,2-cyclohexanediamine (DACH), tert-butoxide, toluene, 110 ℃, 18 h; b) Miyaura boronization reaction: $Pd(dppf)Cl_2$, KOAc, 1,4-dioxane, 85 ℃; c) Suzuki coupling reaction: $Pd(PPh_3)_4$, K_2CO_3, toluene, 90℃, 12h to afford AnPBrCN and 24 h to afford DPAC-AnPCN. All the reactions mentioned above are protected by nitrogen atmosphere.

The synthetic route to DPAC-AnPCN was shown in Scheme 1. DPAC was decorated on the N-site with bromobenzene group and then get boronated to obtain the precursor DPACB. dBrAn was substituted on one side with benzyl cyanide group via Suzuki coupling reaction to get AnPBrCN. Finally, DPACB was coupled with AnPBrCN to attain target molecule DPAC-AnPCN. The crude product was purified by column chromatography, and then elaborate characterization including mass spectrum (MS), NMR measurement and elemental analysis (EA) were performed to confirm the structure of DPAC-AnPCN. The details of the characterization data are summarized in the Supporting Information (SI).

Thermal properties

Thermal properties of DPAC-AnPCN were examined by thermal gravimetric analysis (TGA) and differential scanning calorimetry (DSC). As shown in Figure 1a, The decomposition temperature (T_d, corresponding to 5% weight loss) of DPAC-AnPCN was 426 °C, indicating that DPAC-AnPCN could endure high temperature and would not go through decomposition during device fabrication and operation. The DSC data of the target molecular was shown in Figure 1b. Upon heating procedure, no obvious exo- or endothermic signal could be seen until the melting point (T_m) occurs at 342 °C. No glass transition temperature (T_g) could be observed in the scan range from 50 °C to 375 °C, demonstrating that DPAC-AnPCN would keep stable morphology which is significant and essential for OLEDs applications.

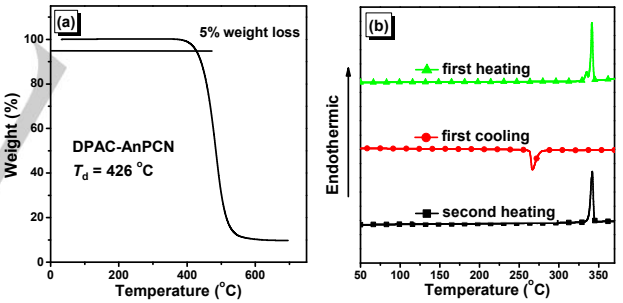

Figure 1. TGA (a) and DSC (b) graphs of **DPAC-AnPCN**. Heating rate: 10 °C·min^{-1}.

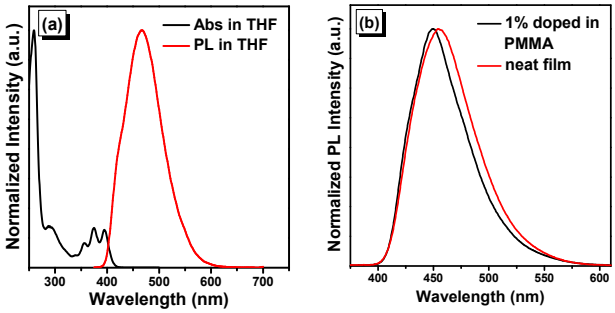

Figure 2. (a) The UV-vis and PL spectra of **DPAC-AnPCN** in dilute THF solution with concentration of 10^{-5} M; (b) PL spectra of **DPAC-AnPCN** in films.

Photophysical properties

The UV/Vis absorption and photoluminescence (PL) spectra of DPAC-AnPCN were recorded in various solvents with different polarities with a dilute concentration of 10^{-5} M. As shown in Figure 2a, the molecule showed sharp absorption peaks at 357 nm, 375 nm and 395 nm in THF, which was attributed to characteristic absorption of anthracene group. Another unstructured trailing absorption peak around 406 nm could be identified to the CT absorption of the molecule. Obvious solvatochromic phenomenon was observed of DPAC-AnPCN in the measurement of emission spectra in different solvents which is shown in 3a. The emission peak of DPAC-AnPCN shifted 100 nm from 438 nm in low-polar solvent n-hexane to 538 nm in high-polar solvent acetonitrile, indicating the strong CT property of the S_1 state. This CT property was well matched the calculation results. The energy level of S_1 of DPAC-AnPCN was calculated to be 2.77 eV, which came from the emission peak of toluene (447 nm). Then DPAC-AnPCN was dispersed into polymethyl mechacrylate (PMMA) with concentration of 1 wt%. The prepared DPAC-AnPCN PMMA doped film showed emission peak at 449 nm and the pure thin film shows at 454 nm. (Figure 2b) Similar emission wavelength implied that little intermolecular interactions worked in the nondoped condition. Both films showed unstructured board emission peak which coordinates with the states in the solvents. Similar with the former work based on anthracene, the phosphorescence of DPAC-AnPCN could hardly be gained with the method tested using spectrometer in frozen 2-methy THF at 77K. The main reason was that the low-positioned T_1 of An group made a narrow band gap between T_1 and S_0. According to the energy gap law, the dominating way of consuming T_1 energy might be nonradiative transition but not the decay from T_1 to S_0. Thus, PtOEP was introduced as a triplet sensitizer followed the reported method.[14] The first vibrational peak of phosphorescence of the molecule was 713 nm, then the T_1 energy level was calculated to be 1.74 eV. (Figure S6) So the phosphorescence originated from the An group, which was the same as other researches of An.

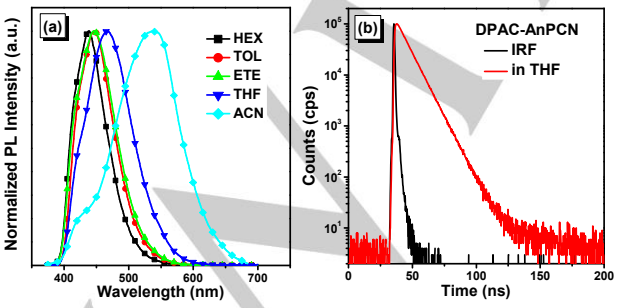

Figure 3. (a) Solvatochromic PL spectra of **DPAC-AnPCN** with increasing polarity of solvents; (b) Transient PL decay of **DPAC-AnPCN** in dilute THF (Concentration: 10^{-5} M).

The transient PL decay of the molecule was further measured and showed in Figure 3b. The molecular show one-exponential PL decays in THF with lifetime of 9.38 ns, and 5.62 ns for its PMMA doped film (Figure S7). No delayed component could be detected, indicating that the emission of the molecule in both states absolutely originated from the directly decay of S_1 state. The PLQYs of the DPAC-AnPCN nondoped and doped films were similar, which are measured to be 65% and 61% using integrating sphere, respectively, indicating that the solid DPAC-AnPCN maintain high radiative transition rate after aggreagating.

Theoretical calculations and electrochemical properties

Theoretical calculations were performed to forecast the properties of DPAC-AnPCN. The optimized configuration of the molecule showed distinctive structure of DPAC moiety, which had a spatial vertical benzene group at the 10 site of acridine. This might make DPAC-AnPCN bigger volume and weaken the intermolecular interactions. This was similar to our former work on DPAC based crystal.[13-a] Then, the HOMO and LUMO distributions of DPAC-AnPCN were calculated by the method of density functional theory (DFT). As shown in Figure S10, the HOMO of the molecule was mostly distributed on the DPAC moiety while the LUMO was mainly distributed on the anthracene and p-benzonitrile moieties. The overlap of HOMO and LUMO was small which indicated the strong intramolecular charge transfer characteristic of DPAC-AnPCN. Then natural transition orbitals (NTO) of the singlet and triplet states were calculated with TD-DFT method to predict the excited states properties of the molecule (Figure S11). The S_1 of DPAC-AnPCN showed obvious charge transfer property. This might mainly owe to the electron-withdrawing ability of the p-benzonitrile group, which lowered the CT energy of DPAC-AnPCN. The calculated T_1 of DPAC-AnPCN was localized state concentrating on anthracene group, which was similar to other reported An-based molecules. The energy levels of S_1 and T_1 of DPAC-AnPCN were calculated to be 3.50 eV and 2.13 eV, respectively, which fitted $2T_1 > S_1$ providing possibility of triplet-triplet annihilation of anthracene group.

The HOMO/LUMO energy levels of DPAC-AnPCN were estimated from cyclic voltammetry (Figure 4). The oxidation potential is originated mainly from electron donor DPAC, while the reduction potential is determined by benzonitrile-substituted anthracene. The oxidation and reduction onset against ferrocenium/ferrocene (Fc^+/Fc) redox couple of DPAC-AnPCN were 0.74 V and -1.74 V, respectively, referring to the calculated HOMO and LUMO energy levels of −5.54 eV and −3.06 eV. The HOMO/LUMO calculation was essential for adjustment of the device structures to achieve suitable energy levels between emitting and transporting materials which could avoid interface emitting and other problems in devices. This is also propitious to improve the device performance.

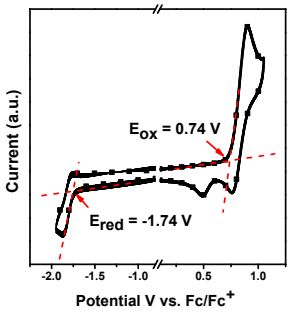

Figure 4. Cyclic voltammograms scans of **DPAC-AnPCN**, the potentials are calibrated against Fc^+/Fc internal standard.

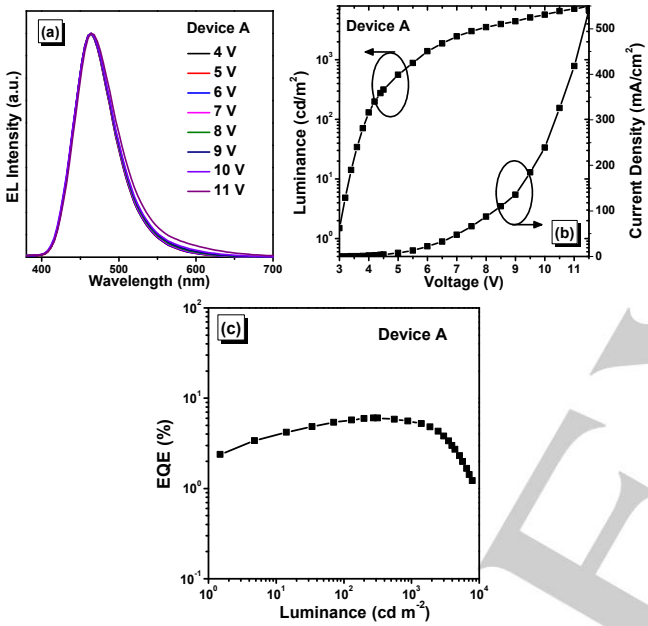

Figure 5. (a) EL spectra of Device A at different driving voltages; (b) Luminance-Voltage-Current Density curves of device A; (c) Luminance-EQE curve of device A.

Table 1. EL data of device based on DPAC-AnPCN.

Device	V[a] (V)	L_{max}[b] (cd·m^{-2})	CE_{max}[c] (cd·A^{-1})	EQE[d] (%)	λ_{EL}[e] (nm)	CIE[f] (x,y)
A	3.0	7929	7.26	6.04	464	(0.15, 0.15)

[a] Turn-on voltage at a luminance of 1 cd·m^{-2}; [b] Maximum brightness; [c] Maximum current efficiency; [d] Maximum external quantum efficiency; [e] EL emission peak at 4V; [f] CIE coordinates at 4V.

Electroluminescent properties

To investigate the electroluminescent (EL) performance of DPAC-AnPCN, we fabricated the nondoped OLEDs devices with structure of indium tin oxide (ITO)/HATCN (6 nm)/TAPC (20 nm)/TCTA (20 nm)/DPAC-AnPCN (20 nm)/TPBi (40 nm)/LiF(1 nm)/Al, where ITO is the anode, hexaazatriphenylenehexacarbonitrile (HATCN) is the hole injecting layer (HIL), TAPC (di-(4-(N,N-ditolyl-amino)-phenyl) cyclohexan) is the hole transporting layer (HTL), TCTA (tris(4-carbazoyl-9-ylphenyl)amine) is the buffer layer, DPAC-AnPCN is the emitting layer (EML), TPBi (1,3,5-tris-(N-phenylbenzimidazol-2-yl)benzene) is the electron transporting layer, LiF is the electron injecting layer and Al is the cathode. The DPAC-AnPCN nondoped device (Device A) showed stable EL emission under various driving voltages and peaked at 464 nm with CIE coordinates of (0.15, 0.15) at 4 V, which accorded with the PL spectra from the nondoped thin films (Figure 5). Device A was turned on at a low voltage of 3 V, which proved that the carrier injection and recombination worked efficiently in the device. The maximum EQE of device A was 6.04%, which is among the best results nondoped fluorescent blue OLEDs. The EQE of device A remained 5.31% at a high luminescence of 1000 cd m^{-2} (Table S2) with a small efficiency roll-off, which fitted the original intention of introducing DPAC group. Further, we also fabricated doped device for DPAC-AnPCN (device B) and adjusted the device structure. After optimizing the thickness of the carrier transporting layers and changing the host materials with modified doping concentration, the best result of device B was gained with the structure of ITO/HATCN (6 nm)/TAPC (25 nm)/TCTA (15 nm)/CBP:DPAC-AnPCN-30% (20 nm)/TPBI (40 nm)/LiF(1 nm)/Al, where 4,4-di(9H-carbazol-9-yl)-1,1-biphenyl (CBP) was the chosen host material for DPAC-AnPCN, and the doping concentration was optimized to be 30% to reach the best performance. The doped device also shows stable deep blue emission peak at 452 nm with CIE coordinates of (0.15, 0.09). Device B achieved a maximum EQE of 5.99% and remains 3.32% at 1000 cd m^{-2} (Figure S9, Table S2). Nearly half of the EQE rolled at high luminescence, which was mainly because that the accumulated excitons were quenched or consumed rather than emit. In consideration of the efficiency roll-off behaviors of the nondoped and doped devices of DPAC-AnPCN, TTA might happen to explain the phenomenon. The TTA process might be effective at low voltage which contributed to the similar maximum EQE of both devices. But at high voltage of luminescence, DPAC-AnPCN in nondoped device gained much more opportunities to collision than the doped device, resulting in more additional emissive S_1 exitons from TTA process.

Conclusions

In summary, an efficient blue emitter DPAC-AnPCN using DPAC as the donor, substituted anthracene as respective acceptor is synthesized. The PLQYs of the DPAC-AnPCN nondoped and doped films were similar, which are measured to be 65% and 61%. The doped device shows a stable deep blue emission peaking at 452 nm with CIE coordinates of (0.15, 0.09). The maximum EQE is 5.99% and remains 3.32% at 1000 cd m^{-2}. The

nondoped device based on DPAC-AnPCN shows a maximum EQE of 6.04% with the CIE coordinates of (0.15, 0.15). The efficiency roll-off of DPAC-AnPCN nondoped device is rather small at the luminance of 1000 cd m^{-2} remaining an EQE of 5.31%. The introduction of DPAC moiety weakens the intermolecular interactions and restrains the aggregation quenching effect. This provides promising molecule design strategies of materials for nondoped blue OLED devices. This result is among the best of nondoped blue fluorescent OLEDs. We believe that our work is valuable for further scientific researches and practical applications such as lightings and display technologies.

Experimental Section

General information

All the reagents and solvents used for the syntheses were purchased from Aldrich and Acros and used as received.

Synthetic procedures

Synthesis of DPACBr

In a 250 mL round flask, a mixture of DPAC (6.67 g, 20 mmol), 1-bromo-4-iodobenzene (8.49 g, 30 mmol), copper(I) iodide (190 mg, 1 mmol), DACH (1.20 ml, 10 mmol), sodium tert-butoxide (2.88 g, 30 mmol) and 100 ml toluene were stirred and refluxed at 110 °C for 12 hours under nitrogen protection. Then the mixture was cooled to room temperature and poured into 100 mL water and extract with dichloromethane (DCM). Then the organic layer was separated and combined. After evaporating the solvent, the residue was further purified by column chromatography with petroleum ether/DCM (4:1, v/v) as the eluent. Finally, the crude product was recrystallized from ethanol to afford white solid. (6.93 g, yield: 71%). ^{1}H NMR (500 MHz, DMSO-D_6, 25 °C, TMS) δ (ppm): 7.83 (d, *J* = 8.5 Hz, 2H), 7.33 (t, *J* = 7.3 Hz, 4H), 7.28 (t, *J* = 7.1 Hz, 2H), 7.10 (t, *J* = 7.1 Hz, 2H), 7.03 (d, *J* = 8.5 Hz, 2H), 6.93 (d, *J* = 7.6 Hz, 2H), 6.90 (d, *J* = 7.5 Hz, 4H), 6.78 (d, *J* = 7.7 Hz, 2H), 6.35 (d, *J* = 8.1 Hz, 2H); MALDI-TOF MS (mass *m/z*): calcd for $C_{31}H_{22}BrN$, 487.09; found, 487.61 [*M*+].

Synthesis of DPACB

In a 250 mL round flask, a mixture of DPACBr (5.86 g, 12 mmol), bis(pinacolato)diboron (6.10 g, 24 mmol), 1,1'-bis[(diphenylphosphino)ferrocene]dichloropalladium $PdCl_2(dppf)_2$ (288 mg, 0.36 mmol), potassium acetate (3.54 g, 36 mmol) and 100 ml dioxane were stirred and refluxed at 85 °C for 24 hours under nitrogen protection. The reaction mixture was extracted with DCM and further purified by column chromatography using petroleum ether/DCM (2:1 v/v) as eluent to attain product as white solid. (2.57g, yield: 40%). ^{1}H NMR (500 MHz, DMSO-D_6, 25 °C, TMS) δ (ppm): 7.92 (d, *J* = 6.5 Hz, 2H), 7.31 (dt, *J* = 20.6, 5.7 Hz, 6H), 7.11 (d, *J* = 6.4 Hz, 2H), 7.07 (t, *J* = 6.4 Hz, 2H), 6.91 (t, *J* = 6.4 Hz, 6H), 6.78 (d, *J* = 6.2 Hz, 2H), 6.31 (d, *J* = 6.6 Hz, 2H), 1.34 (s, 12H); MALDI-TOF MS (mass *m/z*): calcd for $C_{31}H_{34}BNO_2$, 535.27; found, 535.91 [*M*+].

Synthesis of AnPBrCN

In a 100 mL round flask, a mixture of 9,10-dibromoanthracene (3.36 g, 10 mmol), (4-cyanophenyl)boronic acid (1.48 g, 10 mmol), K_2CO_3 (5.52 g, 40 mmol), 20 mL distilled water, 40 mL toluene and $Pd(PPh_3)_4$ (230 mg, 0.20 mmol) was added and refluxed at 90 °C under nitrogen atmosphere for 18 hours. The mixture was poured into water to quench the reaction and then extracted with DCM, the organic layer was collected and combined. After evaporation of the solvent, the residue was purified by column chromatography by using petroleum ether/DCM (4:1, v/v) as eluent to afford greenish solid. (1.97 g, yield: 55%). ^{1}H NMR (500 MHz, DMSO-D_6, 25 °C, TMS) δ (ppm): 8.66 (d, *J* = 8.9 Hz, 2H; Ar H), 7.92 (m, 2H; Ar H), 7.64 (ddd, *J* = 8.9 Hz, 6.4 Hz, 1.1 Hz, 2H; Ar H), 7.56 (m, 2H; Ar H), 7.52 (d, *J* = 8.7 Hz, 2H; Ar H), 7.44 (m, 2H; Ar H). MALDI-TOF MS (mass *m/z*): calcd for C21H12BrN, 357.02; found, 358.01 [*M*+].

Synthesis of DPAC-AnPCN

In a 100 mL round flask, a mixture of AnPBrCN (1.32 g, 4 mmol), DPACB (2.14 g, 4 mmol), K_2CO_3 (5.52 g, 40 mmol), 20 mL distilled water, 40 mL toluene and $Pd(PPh_3)_4$ (230 mg, 0.2 mmol) was added and refluxed at 90 °C under nitrogen atmosphere for 24 hours. The mixture was poured into water to quench the reaction and then extracted with DCM, the organic layer was collected and combined. After evaporation of the solvent, the residue was purified by column chromatography by using petroleum ether/DCM (1:1, v/v) as eluent to afford white solid. (2.47 g, yield: 90%). ^{1}H NMR (500 MHz, DMSO-D_6, 25 °C, TMS) δ (ppm): 8.16 (d, *J* = 8.0 Hz, 2H; Ar H), 7.75 (d, *J* = 7.7 Hz, 4H; Ar H), 7.71 (d, *J* = 7.8 Hz, 2H; Ar H), 7.54 (dd, 6H; Ar H), 7.20-7.39 (m, 10H; Ar H), 6.92-7.06 (m, 6H; Ar H), 6.85 (d, *J* = 8.0 Hz 2H; Ar H), 6.71 (d, *J* = 8.4 Hz, 2H); ^{13}C NMR (125 MHz $CDCl_3$, 25 °C, TMS): δ= 146.37, 144.32, 144.23, 142.27, 140.21, 138.67, 137.13, 134.95, 133.40, 132.32, 131.44, 130.45, 130.09, 129.74, 129.44, 127.68, 126.99, 126.26, 125.85, 125.55, 120.39, 118.55, 114.15, 111.50 (ppm). MALDI-TOF MS (mass *m/z*): calcd for $C_{52}H_{34}N_2$, 686.27; found, 686.9 [*M*+]. Anal. Calcd (%) for $C_{52}H_{34}N_2$: C, 90.93; H, 4.99; N, 4.08. Found: C, 90.81; H, 5.03; N, 4.16.

Acknowledgements

This research is supported by the National Basic Research Program of China (Grant No. 2016YFB0401001), National Natural Science Foundation of China (91833304,21774047) and the Jilin Provincial Science and Technology Department (20180201084GX) and the Fundamental Research Funds for the Central Universities.

Keywords: anthracene • blue emission • high solid-state efficiency • low efficiency roll-off • OLED

[1] C. W. Tang, S. A. VanSlyke, *Appl. Phys. Lett.* **1987**, *51*, 913.

[2] (a) M. Zhu, C. Yang, *Chem. Soc. Rev.* **2013**, *42*, 4963; (b) X. Zhan, Z. Wu, Y. Lin, Y. Xie, Q. Peng, Q. Li, D. Ma, Z. Li, *Chem. Sci.* **2016**, *7*, 4355; (c) B. Chen, B.Liu, J. Zeng, H. Nie, Y. Xiong, J. Zou, H. Ning, Z. Wang, Z. Zhao, B. Z. Tang, *Adv. Funct. Mater.* **2018**, *28*, 1803369.

[3] (a) S. Reineke, F. Lindner, G. Schwartz, N. Seidler, K. Walzer, B. Luessem, K. Leo, *Nature* **2009**, *459*, 234; (b) X. Sun, J. Li, H. Liu, P. Lu, *Actc Polym. Sin.* **2018**, *2*, 284; (c) D. Zhang, L. Duan, Y. Zhang, M. Cai, D. Zhang, Y. Qiu, *Light: Sci. Appl.* **2015**, *4*, e232.

[4] (a) X. Sun, L. Zhao, X. Han, H. Liu, Y. Gao, Y. Tao, H. Zhang, B. Yang, P. Lu, *Molecules* **2018**, *23*, 190; (b) Y. Xu, X. Liang; X. Zhou, P. Yuan, J. Zhou, C. Wang. B. Li, D. Hu, X. Qiao, X. Jiang, L. Liu, S. J. Su, D. Ma, Y. Ma, *Adv. Mater.* **2019**, *31*, 1807388.

[5] (a) M. A. Baldo, D. F. O'Brien, Y. You, A. Shoustikov, S. Sibley, M. E. Thompson, S. R. Forrest, *Nature* **1998**, *395*, 151; (b) M. A. Baldo, D. F. O'Brien, M. E. Thompson, S.R. Forrest, *Phys. Rev. B: Condens. Matter Mater. Phys.* **1999**, *60*, 14422.

[6] (a) C. Adachi, M. A. Baldo, M. E. Thompson, S. R. Forrest, *J. Appl. Phys.* **2001**, *90*, 5048; (b) K. S. Yook, J. Y. Lee, *Adv. Mater.* **2012**, *24*, 3169; (c) Y. Tao, C. Yang, J. Qin, *Chem. Soc. Rev.* **2011**, *40*, 2943.

[7] (a) H. Uoyama, K. Goushi, K. Shizu, H. Nomura and C. Adachi, *Nature*, **2012**, *492*, 234; (b) H. Nakanotani, T. Higuchi, T. Furukawa, K. Masui, K. Morimoto, M. Numata, H. Tanaka, Y. Sagara, T. Yasuda and C. Adachi, *Nat. Commun.*, **2014**, *5*, 4016; (c) S. Hirata, Y. Sakai, K. Masui, H. Tanaka, S. Y. Lee, H. Nomura, N. Nakamura, M. Yasumatsu, H. Nakanotani, Q. Zhang, K. Shizu, H. Miyazaki, C. Adachi, *Nat. Mater.* **2015**, *14*, 330.

[8] (a) X. Tang, Y. Tao, H. Liu, F. Liu, X. He, Q. Peng, J. Li, P. Lu, *Luminescence. Front. Chem.* **2019**, *7,* 373 (b) Q . Zhang, J. Li, K. Shizu, S. Huang, S. Hirata, H. Miyazaki, C. Adachi, *J. Am. Chem. Soc.* **2012**, *134*,14706.

[9] (a) T.-A. Lin, T. Chatterjee, W.-L. Tsai, W.-K. Lee, M.-J. Wu, M. Jiao, K.-C. Pan, C.-L. Yi, C.-L. Chung, K.-T. Wong, C.-C. Wu, *Adv. Mater.* **2016**, *28*, 6976; (b) D. R. Lee, B. S. Kim, C. W. Lee, Y. Im, K. S. Yook, S.-H. Hwang, J. Y. Lee, *ACS Appl. Mater. Interfaces* **2015**, *7*, 9625; (c) L. Yu, Z. Wu, G. Xie, C. Zhong, Z. Zhu, H. Cong, D. Ma, C. Yang, *Chem. Commun.* **2016**, *52*, 11012.

[10] (a) Y. Li, Z. Xu, X. Zhu, B. Chen, Z. Wang, B. Xiao, J. W. Y. Lam, Z. Zhao, D. Ma, B. Z. Tang, *ACS Appl. Mater. Interfaces* **2019**, *11*, 17592; (b) Z. Li, C. Li, Y. Xu, N. Xie, X. Jiao, Y. Wang, *J. Phys. Chem. Lett.* **2019,** *10*, 842; (c) Y. Yuan, J.-X. Chen, F. Lu, Q.-X. Tong, Q.-D. Yang, H.-W. Mo, T.-W. Ng, F.L. Wong, Z.-Q. Guo, J. Ye, Z. Chen, X.-H. Zhang, C.-S. Lee, *Chem. Mater.* **2013,** *25*, 4957.

[11] (a) R. Kim, S. Lee, K.-H. Kim, Y.-J. Lee, S.-K. Kwon, J.J. Kim, Y.-H. Kim, *Chem. Commun.* **2013**, *49*, 4664; (b) J.-Y. Hu, Y.-J. Pu, F. Satoh, S.Kawata, H. Katagiri, H. Sasabe, J. Kido, *Adv. Funct. Mater.* **2014**, *24*, 2064.

[12] (a) J.-Y. Hu, Y.-J. Pu, Y. Yamashita, F. Satoh, S. Kawata, H. Katagiri, H. Sasabe, J. KIdo, *J. Mater. Chem. C*, **2013**, 1, 3871; (b) H. Liu, L. Kang, J. Li, F. Liu, X. He, S. Ren, X. Tang, C. Lv, P. Lu, *J.Mater. Chem. C*, **2019**, *7,* 10273.

[13] (a) X. He, T. Shan, X. Tang, Y. Gao, J. Li, B. Yang, P. Lu, *J.Mater. Chem. C*, **2016**, *4*, 10205; (b) J. Lee, N. Aizawa, M. Numata, C. Adachi, T. Yasuda, *Adv. Mater.* **2017**, *29*, 1604856; (c) T.-A. Lin, T. Chatterjee, W.-L. Tsai, W.-K. Lee, M.-J. Wu, M. Jiao, K.-C. Pan, C.-L. Yi, C.-L. Chung, K.-T. Wong, *Adv. Mater.* **2016**, *28*, 6976.

[14] (a) L. Yao, Y. Pan, X. Tang, Q. Bai, F. Shen, F. Li, P. Lu, B. Yang, Y. Ma, *J. Phys. Chem. C* **2015**, *119*, 17800; (b) M. Aydemir, G. Haykır, A. Battal, V. Jankus, S. K. Sugunan, F. B. Dias, H. A. Attar, F. Türksoy, M. Tavaslı, A. P. Monkman, *Org. Electron.* **2016**, *30*, 149.

10.1002/asia.201901376

WILEY-VCH

Entry for the Table of Contents

FULL PAPER

D-A-A' type molecule **DPAC-AnPCN** shows high PLQY of 65% in its pure film and strong charge transfer properties. The nondoped device with **DPAC-AnPCN** as emitter achieves a maximum EQE of 6.04% with small efficiency roll-off, which EL peaks at 464 nm with CIE coordinates of (0.15, 0.15).This meets well with the criteria of pure blue OLEDs.

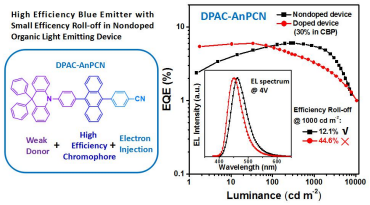

*X. He, S. Ren, H. Liu, S. Zhao, F. Liu, C. Du, J. Min, P. Lu**

Page No. – Page No.

Efficient Nondoped Pure Blue Organic Light-emitting Diodes Based on Anthracene and 9,9-diphenyl-9,10-dihydroacridine Derivative